Cell Reports, Volume *22*

Supplemental Information

Functional Principles of Posterior Septal Inputs to the Medial Habenula

Yo Otsu, Salvatore Lecca, Katarzyna Pietrajtis, Charly Vincent Rousseau, Païkan Marcaggi, Guillaume Pierre Dugué, Caroline Mailhes-Hamon, Manuel Mameli, and Marco Alberto Diana

SUPPLEMENTAL INFORMATION

SUPPLEMENTAL EXPERIMENTAL PROCEDURES

All procedures involving experimental animals were performed in accordance with the Directive 2010/63/EU, and local ethics committee guidelines. All efforts were made to minimize animal suffering and the number of animals used.

Slice preparation

All mice used were more than 3 months old. Coronal brain slices (300 µm) including the MHb and the dorsal hippocampus (Fig.2) were prepared from either C57/B6 mice, GluN2KO mice or their control littermates (C57/B6 genetic background), VGluT2-Cre mice (C57/B6 background), or, finally, from Thy1-ChR2 mice (line 18; Wang et al., 2007). Following deep anesthesia with isoflurane, the brain was quickly removed in an ice-cold bicarbonate-buffered (BBS) solution containing the following (mM): 116 NaCl, 2.5 KCl, 1.25 NaH_2PO_4, 25.7 $NaHCO_3$, 30 glucose, 2 $CaCl_2$, 1.5 $MgCl_2$, and 5×10^{-5} minocycline (bubbled with 95% O_2, 5% CO_2). Slices were cut using a vibrating blade microtome (Campden model 7000smz2) in an ice-cold solution containing the following (mM): 130 K-gluconate, 15 KCl, 2 EGTA, 20 HEPES, 25 glucose, 1 $CaCl_2$, 6 $MgCl_2$ and 0.05 D-(−)-2-amino-5-phosphonovaleric acid (D-APV) (pH 7.4 with NaOH), and were then transiently immersed in a modified BBS, as follows (mM): 225 D-mannitol, 2.5 KCl, 1.25 NaH_2PO_4, 25 $NaHCO_3$, 25 glucose, 1 $CaCl_2$, 6 $MgCl_2$ and 0.05 D-APV (25°C, bubbled with 95% O_2, 5% CO_2). Finally slices were transferred to warm BBS (32°-34°C) for the rest of the experimental day.

Electrophysiology

For electrophysiological recordings, slices were moved to a recording chamber mounted on an upright Slicescope (Scientifica, Uckfield, UK) and continuously perfused with bubbled BBS (~2 ml/min; 30–34°C).
We recorded neurons located exclusively in the ventral part of the MHb (vMHb). Cells were visualized with a combination of Dodt contrast, and an on-line video contrast enhancement. Tight-seal cell-attached (CA), whole-cell (WC), and loose cell-attached (LCA) recordings were performed with an EPC-10 double amplifier (Heka Elektronik, Lambrecht/Pfalz, Germany) run by PatchMaster software (Heka). MHb cells could be easily identified in the transmitted deep red light (~750 nm) with which slices were visualized using a CoolSnap HQ^2 CCD camera (Photometrics, Trenton, NJ) run by MetaMorph (Universal Imaging, Downington, PA). For WC recordings, patch pipettes (resistance 2.5-4MΩ) were filled with an intracellular solution containing (mM): 150 $CsMeSO_3$ (Sigma), 10 TEA·Cl, 1 $CaCl_2$, 4.6 $MgCl_2$, 10 HEPES, 10 K_2-creatine phosphate (Calbiochem), 0.5 EGTA , 4 Na_2-ATP, 0.4 Na_2-GTP, 0.1 spermine and 2 QX-314, pH 7.35 with CsOH (~300 mOsm), sometimes supplemented with a morphological dye (5µM Alexa 488, Invitrogen) to check cell morphology. For current clamp recordings (Fig.S2), and experiments examining DCG-IV-induced currents in WC, the intracellular solution contained as follows (mM): 150 K-Gluconate, 4 NaCl, 10 Hepes, 10 K_2-phosphocreatine, 0.1 K_3EGTA, 6 Mg_2ATP, 0.4 NaGTP. In the WC configuration, series resistance was partially compensated (max 65%), whereas liquid junction potentials were not corrected. Loose Cell Attached (LCA; seal resistance: 15-20 MΩ) recordings were performed at a holding potential at -60 mV, with pipettes of resistance comprised between 2.5 and 5 MΩ) filled with an HEPES-buffered solution (HBS) containing (mM): 130 NaCl, 2.5 KCl, 1.25 NaH_2PO_4, 30 glucose, 2 $CaCl_2$, 1.5 $MgCl_2$, 10 HEPES, pH 7.35 with NaOH (~300 mOsm). Currents were filtered at 10 kHz and sampled at 10-40 kHz. Stimulation electrodes were patch pipettes filled with ACSF and put in the vicinity of MHb cell dendrites to activate the excitatory inputs. The MHb lacks a spatially precise, reciprocal organization of incoming axonal fibers and postsynaptic dendrites. As a consequence, after establishing the WC configuration the search for synaptic responses had variable duration, ranging from a few seconds to several minutes. When found, transmission originated from single presynaptic axons (see Fig.2). Excitatory inputs were stimulated either with individual pulses (7-22 V, 200 µs, biphasic), or with 5 stimuli at 100Hz every 15s for the calcium imaging experiments (Fig.4), or with trains consisting of 10 stimuli at 200 Hz every 10-20 sec for NMDA current examination (Fig.5B&D). This latter protocol closely reproduced the average intra-burst firing frequency of PS neurons (Fig.1). Furthermore, this stimulation pattern was necessary in order to maximize synaptic summation, reduce inter-trial variability, and thus minimize the number of trial repetitions at potentials where recordings of MHb cells rapidly deteriorated (between -20mV and +10mV). In all *ex vivo* experiments where glutamatergic synaptic currents were evoked electrically, SR95531 (2-5µM) was added to the bath solution, together with the mGluRII blocker LY341495 (0.5/1µM), the GABAb antagonist CGP55845 (1µM), and the wide spectrum purinergic receptor blocker CGS15943 (0.5µM).

Calcium imaging

Whole-cell patch pipettes were filled with an intracellular solution containing (in mM): 135 $CsMeSO_3$ (Sigma), 4.6 $MgCl_2$, 10 HEPES, 10 K_2-creatine phosphate (Calbiochem), 4 Na_2-ATP, 0.4 Na_2-GTP, 2 QX-314, pH 7.35 with CsOH (~300 mOsm) and supplemented with a morphological (10µM Alexa 594, Invitrogen) and a calcium-

sensitive dye (500 µM Fluo-5F, Invitrogen). Cells were voltage-clamped at -60 mV in the WC configuration via a Multiclamp700B amplifier (Molecular devices, Sunnyvale, USA). The series resistance was partially compensated (~60%). WC currents were filtered at 1-2 kHz, and sampled at 10 kHz. Imaging was done at 32-34°C (Single Channel Heater Controller, Warner Instruments) in the continuous presence of (µM): 50 D-APV, 5 SR95531, 1 CGP55845 and 0.5 CGS15943, 0.25 LY341495. Calcium signals in MHb cell dendrites were monitored by two-photon random-access microscopy using acousto-optic deflector (AOD)-based scanning (Otsu et al., 2014). In this instrument, both X and Y scannings are operated by acousto-optic deflectors (AODs). These non-mechanical beam-steering devices (A-A Opto-Electronic) can redirect the laser beam in 10µs. To operate the AODs and run the scanning procedures, a custom-made user interface was programmed in LabView (National Instruments). The AOD acoustic frequency drive was generated by a Direct Digital Synthesizer and a fast (10ns) power amplifier (A-A Optoelectronics). Two-photon excitation was produced by an infrared Ti-Sa pulsed laser tuned to 825nm by a Chamaelon-XR (Coherent) coupled to a microscope (Slicescope, Scientifica). The microscope was equipped with a 25×/0.95NA objective (LUMPlanFL/IR, Leica microsystems). Fluorescence photons were detected by cooled AsGaP H10769PA–40 photomultipliers (Hamamatsu) in the transfluorescence and epifluorescence pathways, with a 641/75 nm bandpass filter (Semrock) to see the cell morphology, and a 510/84 nm bandpass filter (Semrock) to acquire calcium signals (Otsu et al., 2014).
Firstly, a synaptic input was searched for by moving the stimulation pipette in the area surrounding the recorded cell, using short stimulation trains (5 pulses at 100Hz). Once found the input, regions of interest (ROIs) were chosen in such a way to cover as large a dendritic area as possible in the available field of view. If no calcium increase was detected, the focus plane was changed and new ROIs on other sections of the dendritic processes were set until a calcium signal was clearly recorded. Calcium signals were acquired for 100-200ms before electrical stimulation of the incoming septal input and, for 1.8-2s following stimulation onset. Dwell times of 20-30µs per point were used. Calcium signals were sampled every 0.9-1.2ms.
To perform stable, long-duration multipoint acquisitions, registration of the field of view was implemented online between each episode of stimulation by 3D correlation between the image of a small field and a previously acquired 3D stack of the same region. Stimulation-induced calcium transients were acquired every 15s for 10/15 min before applying NASPM (20-50µM). The effect of NASPM was monitored in the following 10-15minutes.
For data analysis, relative fluorescence was expressed as ΔG/R, i.e. variations in Fluo-5F signals change (ΔG) divided by calcium-independent Alexa 594 red fluorescence (R). This ratiometric method scales the calcium fluorescence signal to the volume of the imaged compartment, yielding a measurement of the dye-bound cytoplasmic calcium concentration independent of dendritic geometry (Otsu et al., 2014). Image analysis was performed in Igor (Wavemetrics, Lake Oswego, USA).

Ex vivo and _in vivo_ optogenetics

Stereotactic injections

All optogenetic experiments were performed on adult (≥ 3 month-old) VGluT2-Cre mice (Borgius et al., 2010) obtained via the European Mouse Mutant (EMMA) Archive. Mice were anesthetized with an intraperitoneal injection of ketamine-xylazine (200 and 10 mg/kg, respectively) and placed inside a stereotactic apparatus (Kopf Instruments, Tujunga, CA). An AAV2/1-EF1α-DIO.hChR2(H134R).eYFP virus, based on Addgene plasmid 20298 and produced at the Laboratory of Gene Therapy (INSERM UMR 1089, Nantes, France), was injected in the posterior septum, at the following coordinates: Bregma ML: 0.0mm ; AP, -0.13-0.2mm; DV, -2.6mm. For the *in vivo* control experiments described in Fig.7, posterior septal neurons were transfected using an AAV2/1-EF1α-DIO.eYFP virus, based on Addgene plasmid 27056, and produced by the Vector Core facility of the University of Pennsylvania.
Injections were performed using pipettes pulled from graduated capillaries, at a rate of 100-150 nl/min for a total volume of around 300/500nL. All optogenetic experiments were all performed at least four weeks after viral injection.
Concerning cannula implantations for *in vivo* experiments, four weeks after transfection of posterior septal cells with either a hChR2-eYFP or an eYFP expressing virus, VGluT2-Cre animals were re-anaesthetized with ketamine-xylazine (100 and 5 mg/kg) and placed in a stereotactic frame. Once exposed, the skull was cleaned with H_2O_2 and covered with a layer of Super Bond C&B (Morita, Dietzenbach, Germany). A craniotomy was performed and an optic fiber (200 µm, 0.53 NA, 3mm) housed inside a connectorized implant (M3, Doric Lenses, Quebec, Canada) was lowered over the MHb (Bregma -1.5 AP, +0.0 ML,-2.2/-2.5 DV). The craniotomy was covered with a drop of warm agarose gel (2%), and the implant was secured with dental acrylic (Pi-Ku-Plast HP 36, Bredent, Senden, Germany). The skin was stitched at the rear and front of the implant and the animal was allowed to recover on a heating pad. Mice were allowed to recover for at least 5 days before testing.

Ex vivo optogenetics stimulations

The brief (1-2 ms long) flashes of blue light used to evoke leEPSCs were provided by triggering a 470 nm-wavelength LED (Thorlabs, Maisons-Laffitte, France) coupled to the slice chamber via the epifluorescence

pathway of the microscope. The effect of optogenetic stimulation in slices was studied by recording cells in either the WC, or the LCA configuration as described.

In vivo optogenetic experiments

The custom optical system used for fiber optic light delivery in freely moving mice was described previously (Giber et al., 2015). Briefly, the beam generated by a 473 nm DPSS laser (LRS-0473-PFM-00100-03, Laserglow Technologies, Toronto, Canada) was passed through an acousto-optic tunable filter (AOTFnC-400.650-TN, AA Opto-Electronic, Orsay, France) controlled by a multi digital synthesizer (MDS4C-D66-22-74.158-RS). The first order beam exiting the AOTF was bounced on mirrors and directed into the core of a fiber optic patchcord (200 μm, 0.37NA) through a custom table-top rotary joint (Doric). The patchcord (1.6 m) was connected to the mouse cannula and allowed to rotate passively. With adequate beam alignment, rotations induced power fluctuations of less than 5% at the fiber output.
During each session, mice movement was filmed continuously via a CCD camera (Scout scA640-74, Basler, Ahrensburg, Germany). All aspects of the experiment (photostimulation waveform generation, MDS and LED control, video recordings) were controlled using LabVIEW (National Instruments Corporation, Austin, TX).

Open field test.
Cannula-implanted mice were housed in individual cages. Before being introduced into the arena, the animals were allowed to get acquainted to the experimental room and its light conditions (~30lux) for at least 60min. Mice were then connected to the patchcord, and allowed to move freely in a gray, round open field arena (38cm diameter, 15cm wall height, Noldus, Wageningen, Holland) while being filmed. After 5min of free movement in the arena, optogenetic stimulation was activated for 3min using either a continuous 20Hz train, or alternate laser-on (20Hz, 1s) / laser-off (2s) periods (see results). After end of stimulation, the mice were left in the arena for 5 more minutes. The periodic protocol was also examined on mice following (minimum 90min) intraperitoneal injection of LY341495 (1-4mg/Kg) dissolved in saline (9% NaCl in distilled water; Scofield et al., 2015). Injection of LY341495 did not *per se* affected locomotion. Indeed, the total distances travelled by AAV2/1-DIO.hChR2-eYFP injected VGluT2-Cre mice in the minute preceding laser onset were 326.5±33.4cm and 255.9±40.4cm for the intermittent protocol in naïve (i.d.: not i.p. injected) and LY341495 injected mice ($p=0.11$), respectively.
Individual experimental sessions were performed at least at one week distance. Movies were analyzed off-line with Ethovision (Noldus). Raw data were then exported, and further analyzed in Igor Pro 5.0 (Wavemetrics, Lake Oswego, USA). Total distances traveled in the minute before laser stimulation onset, and between 30s and 90s following light onset were quantified, and statistically compared between the different conditions indicated in the text.

Elevated plus maze.
The Elevated Plus Maze (EPM) test was performed using a standard apparatus (arm length: 65cm x 65cm, height: 47.5cm; Imetronic, Pessac, France) with transparent plastic walls delimiting the enclosed sections. Mice got accustomed to the experimental room light level in their home cage for at least 1 hour prior to testing. The laser-connected patchcord was then screwed to the implanted cannula, and the mouse was allowed to freely explore the EPM for 13 minutes. Alternated light stimulation (1s/on, 2s/off) was activated between minutes 5 and 8 during the test. Videos were analyzed off-line with Ethovision (Noldus).

Marble burying.
For this test, 3 rows of 8 steel marbles (diameter: 1cm) were placed on fresh bedding in a transparent plastic box (44cm long, 28cm large). Mice got accustomed to the experimental room light level in their home cage for at least 1 hour prior to testing, and 15 more minutes following fixation of the patchcord to the implanted cannula. They were then introduced in the box and allowed to roam freely during periodic light trains (1s/on, 2s/off). The number of marbles completely buried after 10 minutes was quantified.

In vivo recordings of posterior septal firing patterns
Mice were anesthetized with isoflurane (Univentor, Malta. Induction: 2%; maintenance: 1-1.5%), and placed in a stereotaxic apparatus (Kopf, Germany). Their body temperature was maintained at 36±1°C using a heating pad (CMA 450 Temperature Controller, USA). The scalp was retracted and one burr hole was drilled above the posterior septum (AP: 0.0–0.2 mm, ML: 0.0–0.1 mm, DV: 2.6–3.1) for the placement of a recording electrode. For identifying MHb-projecting septal neurons with antidromic stimulation, a bipolar concentric electrode was lowered in the MHb (AP: -1.5 mm, ML: 0.3 mm, DV: 2.8 mm), with a 10° inclination in the rostro-caudal axis.
Single unit activity was recorded extracellularly by glass micropipettes filled with 2% pontamine sky blue dissolved in 0.5 M sodium acetate (impedance 3–6 MΩ). Signals were filtered (band-pass 500–5000 Hz), pre-

amplified (DAM80, WPI, Germany), amplified (Neurolog System, Digitimer, UK), and displayed on a digital storage oscilloscope (OX 530, Metrix, USA).
Experiments were sampled on- and off-line by a computer connected to a CED Power 1401 laboratory interface (Cambridge Electronic Design, Cambridge, UK) running the Spike2 software (Cambridge Electronic Design). Single units were isolated and the spontaneous activity was recorded for 5min.
Spontaneous firing rate, percentage of spikes in bursts, mean spikes per burst, mean burst duration, mean intra-burst frequency and coefficient of variation (CV=standard deviation of interspike intervals divided by the mean interspike interval) were determined. Criteria for burst identification were chosen via qualitative analysis of the interspike interval histogram of the recorded cells. We defined as a burst a sequence of action potentials starting when 2 events occurred with an interval smaller than 20ms, and ending when the interval between 2 consecutive spikes exceeded 50ms.
MHb-projecting PS neurons were identified using high frequency collision methods (Glangetas et al., 2013), following antidromic stimulation in the MHb. Stimulation-triggered spikes were considered antidromic if they met the following criteria: 1) constant latency from stimulation onset, 2) high reliability (~100%) of antidromic stimulation at 100Hz, or greater, frequencies, and 3) collision of triggered spikes with spontaneous action potentials occurring in an interval approximately equal to the sum of the refractory period, and of the latency from stimulation.
At the end of each experiment, the electrode placement was marked with an iontophoretic deposit of pontamine sky blue dye (with a negative continuous current of 80 µA during 35 min). To mark electrical stimulation sites, positive current (10µA) was passed through the stimulation electrode for 1min. Brains were then rapidly removed and fixed in a 4% paraformaldehyde solution. The position of the electrodes was then identified on serial sections (60 µm).

Immunohistochemistry
Methods for immunohistochemical staining followed the protocols described in detail previously (Rousseau et al., 2012; Giber et al., 2015).

Tissue fixation. Adult mice were deeply anesthetized with intraperitoneal injections of sodium pentobarbital (60mg/kg), and perfused through the ascending aorta with PBS, followed by 50ml of 4% freshly depolymerized paraformaldehyde in 100mM PBS, pH 7.4, at 4°C. Brains were then dissected and postfixed in 4% paraformaldehyde overnight at 4°C, before embedding in paraffin.

Tissue preparation and labeling. Sections were cut with a thickness of 7µm. After removing paraffin, sections were processed in a decloaking chamber (Biocare Medical, Concord, CA) using a citrate-buffer-based antigen retrieval medium (Biocare Medical) for 20min at 110–115°C. They were then processed in PBS with 15% methanol and 0.3% H_2O_2 to block endogenous peroxidase activity. Aldehyde groups were removed by incubating the sections in sodium borohydride (1%) in PBS. After these treatments, the slices were incubated in a blocking PBS-based solution containing cold-water fish-skin gelatin (0.1%) and Triton X-100 (0.1%). Tissues were then incubated overnight at 4°C with the following primary antibodies: anti-VGluT2 (1:1000; Millipore), anti-GluA1 (1:500; Synaptic Systems), anti-GluA2 (1:500; Synaptic Systems), GluN1 (1:200; Millipore), GluN2A (1:100; Upstate Biotechnology), GluN2B (1:100; BD Transduction Laboratories), chicken anti-GFP (1:1000; Aves Laboratories). Primary antibodies were revealed by incubation for 2hrs with secondary antibodies coupled to either Alexa Fluor-488 (Invitrogen, Saint Aubin, France) or DyLight488, DyLight549, and DyLight649 (1:200 or 1:400; Jackson ImmunoResearch). Sections were finally mounted using Prolong Gold Antifade Reagent (Invitrogen). For all experiments, control sections were incubated without primary antibodies. Images were acquired using a confocal microscope (SP2, Leica Microsystems) with a 25×, and a 40× oil-immersion objective.

Drug application
DCGIV (10µM), DHPG (50µM), and L-AP4 (200µM) were puffed onto the cells. LY341495 was either bath applied (0.25-1µM) in slices, or injected intraperitoneally (1-4mg/Kg) in mice for *in vivo* experiments. All other drugs were bath applied: NBQX (10µM), D-AP5 (50µM), CGP55845 (1µM), CGS15943 (0.5µM), TBOA (100µM), NASPM (50µM), SR95531 (2-5µM), Zn^{2+} (a free concentration of 300nM was obtained by adding 60µM Zn^{2+} and 10mM tricine (Vergnano et al., 2014)); Ro25-6981 (1µM); CIQ (20µM). NBQX, APV, SR95531 and minocycline were from Abcam (Cambridge, UK). DCGIV, DHPG, CGP55845, CGS15943, TBOA, NASPM, L-AP4, LY341495 were from Tocris (Bristol, UK). All other drugs were from Sigma-Aldrich France (Saint-Quentin Fallavier, France). Ro25-6981 was a kind gift of P. Paoletti (IBENS, Paris).

Data analysis
Data analysis was performed with pClamp 10 (Molecular devices), Origin 6.1 software (OriginLab, Northampton, USA), with custom routines written in Igor, and Ethovision.

Statistical analysis

The results are presented as mean ± SEM throughout the manuscript, and in all figures. For statistical analyses, Mann-Whitney U test and Wilcoxon signed-rank test were used as appropriate. Statistical significance was set at 0.05.

Supplemental Figures

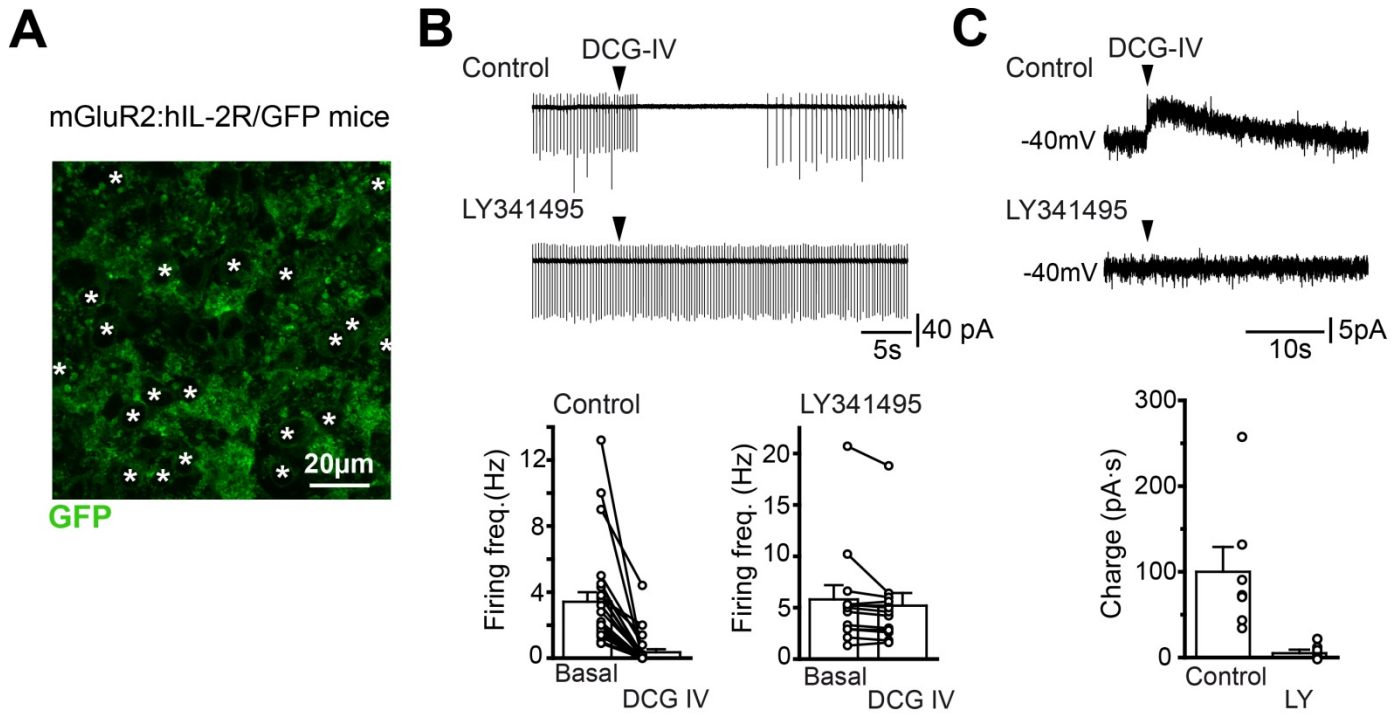

Figure S1 (related to Figure 6). Glutamate group II metabotropic receptors are expressed in MHb neurons and potently reduce spike rate.

A.Immunohistochemical staining for GFP in the MHb of a mouse expressing the human interleukin receptor 2 (hIL-R2) and GFP, under the control of the promoter of the metabotropic glutamate receptor 2 (mGluR2; Watanabe et al., 1998). mGluR2 belongs to the group II metabotropic receptor family (mGluRII). The fluorescence signal was expressed both in presynaptic structures (Yamaguchi et al., 2013), and on the cell membranes of most MHb neurons. A subset of positive cells is highlighted by white asterisks, as an example. **B.** Puffing of the mGluRII agonist DCG-IV (10µM) potently inhibited spike rate in all spontaneously firing MHb cells recorded in the LCA configuration, on average to 7.4±3.1% of the control (range: 0%-56%; n=26; $p<0.001$; see traces for a single neuron on top, and values for all the cells tested in the left bar graph below). DCG-IV action was completely absent when the mGluRII antagonist LY341495 (1µM) was applied in the bath (average firing rate: 93.4±3.7% with respect to control period; n=13; right bar graph). In contrast to mGluRII interfering agents, the group I (mGluRI) agonist DHPG (50µM) produced only a small increase of the firing frequency to 139.9±8.5% of the control, which did not reach statistical significance (n=5; p=0.06; data not shown). Furthermore, the group III (mGluRIII) agonist L-AP4 (200µM) did not induce any modification in action potential rate, which was 97.5±5.0% of the control (n=8; p=0.8; data not shown) during drug application.

C. DCG-IV puffs reliably induced outward currents in MHb cells (total transferred charge: 100.0 ± 28.9pC; n=7) when neurons were recorded in the WC configuration at -40mV. These currents were prevented by LY341495 application (9.7±4.0pC; n=6; p=0.001). See traces from a typical recording on top, and the corresponding graphs for all tested neurons below. Data are represented as mean±SEM.

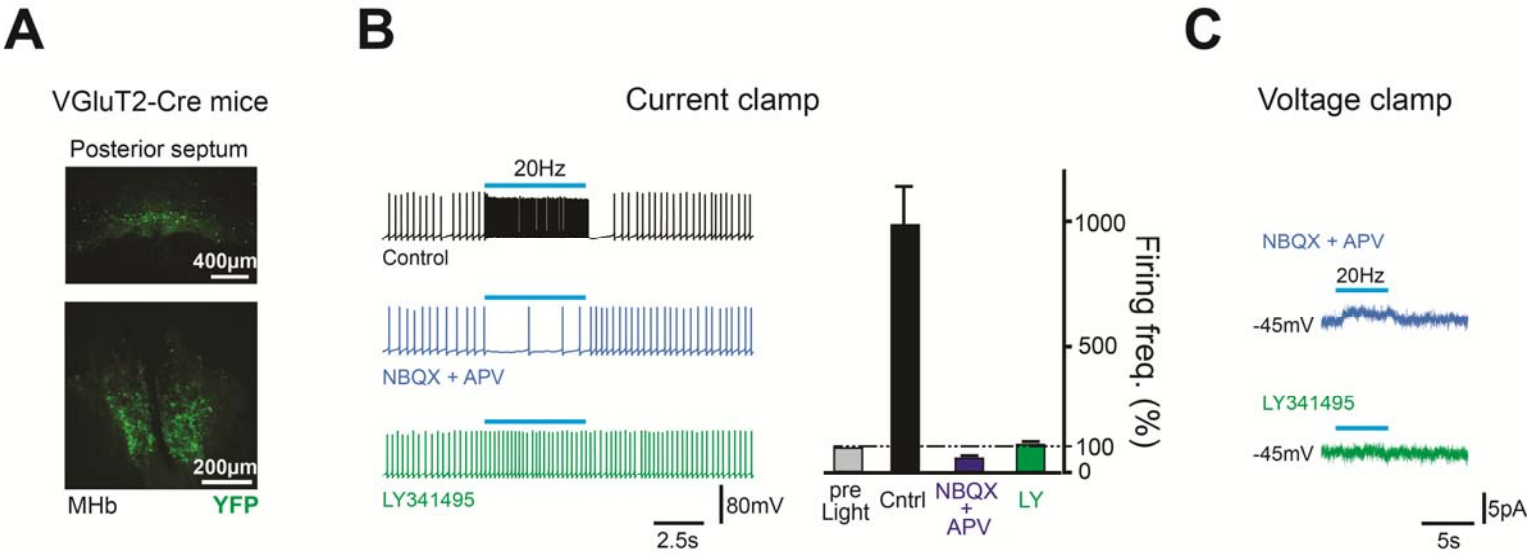

Figure S2 (related to Figure 6). Optogenetically induced modulation of firing in MHb neurons: whole cell recordings.

A. Here we show 2 typical images illustrating the site of injection in the PS (above), and the resulting fluorescence in the MHb (below) of a VGluT2-Cre mouse injected with an AAV2/1-DIO.hChR2-YFP virus. **B.** CC recordings of a MHb cell, in which a 5s-long stimulation train of light pulses at 20Hz (light blue line) triggered a dramatic increase in spike rate, followed by a prominent after-hyperpolarization (black trace, above left). On average, spike rates augmented to 989.2±146.32% of the control (n=17; p=0.0003), whereas average after-hyperpolarizations amounted to 7.0±1.0mV, and led to great inhibition of the action potential frequency, to 40.4±10.8% of the control (n=17; p=0.0007). Co-application of NBQX and APV eliminated the late inhibition completely (average spike rate: 92.3±14.2%; p=0.6; n=14). The block of ionotropic glutamate receptors also revealed a strong decrease of firing during the stimulation train, to 59.0±7.8% of the control (n=15; p=0.002; middle blue trace), which was blocked by LY341495 applications (113.5±8.4%; p=0.08; green trace). The quantification for all the tested cells is in the right bar graph. **C.** In a similar cell as in panel **B**, the stimulation train triggered a small but detectable outward current in the presence of NBQX and APV, amounting to 2.0±0.5pA (n=9; p=0.002; above blue trace), which was blocked by LY341495 (green trace below). Thus, mGluRIIs can indeed be activated by incoming synaptic activity in MHb neurons. These VC recordings were performed at a holding potential of -45mV. Data are represented as mean±SEM.

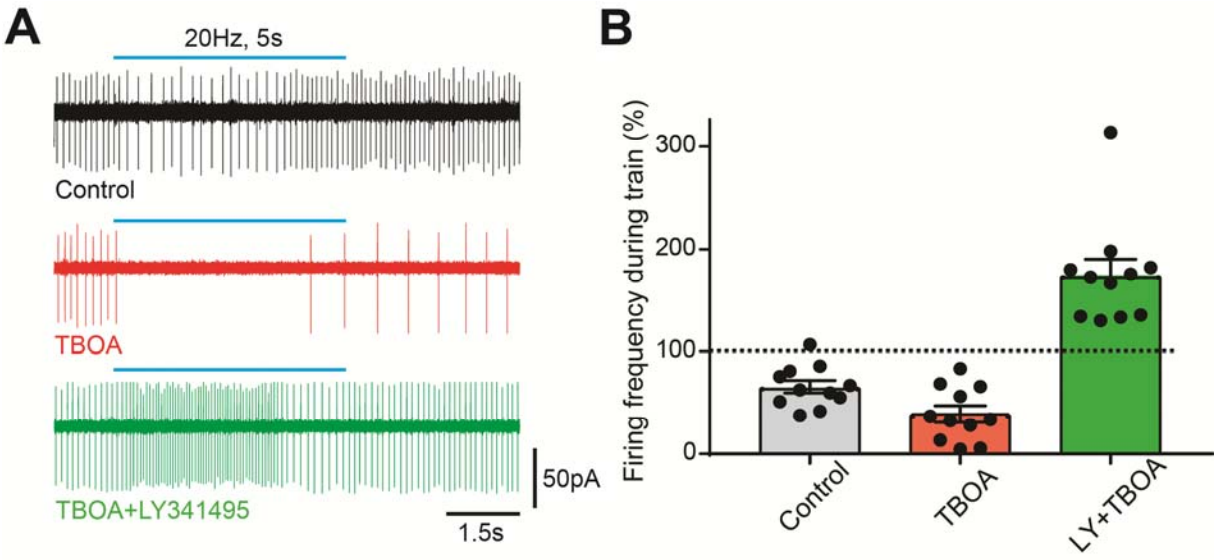

Figure S3 (Related to Figure 6). The glutamate transporter blocker TBOA potentiates the inhibitory effect of mGluRII activation on MHb cell firing.

A. In this MHb cell, a 5s-long light stimulation train at 20Hz (light blue line) reduced the spontaneous spike rate recorded in the LCA configuration (black upper trace), typical for the cell group described in Fig. 6C. Bath application of TBOA (100µM; red middle trace) potentiated the inhibitory effect. Application of the mGluRII antagonist LY341495 completely blocked the inhibition, highlighting an underlying potentiation probably due to mGluRI receptors (green lower trace). The effect of TBOA is quantified for all recorded cells in the bar graph in **B**. Data are represented as mean±SEM.

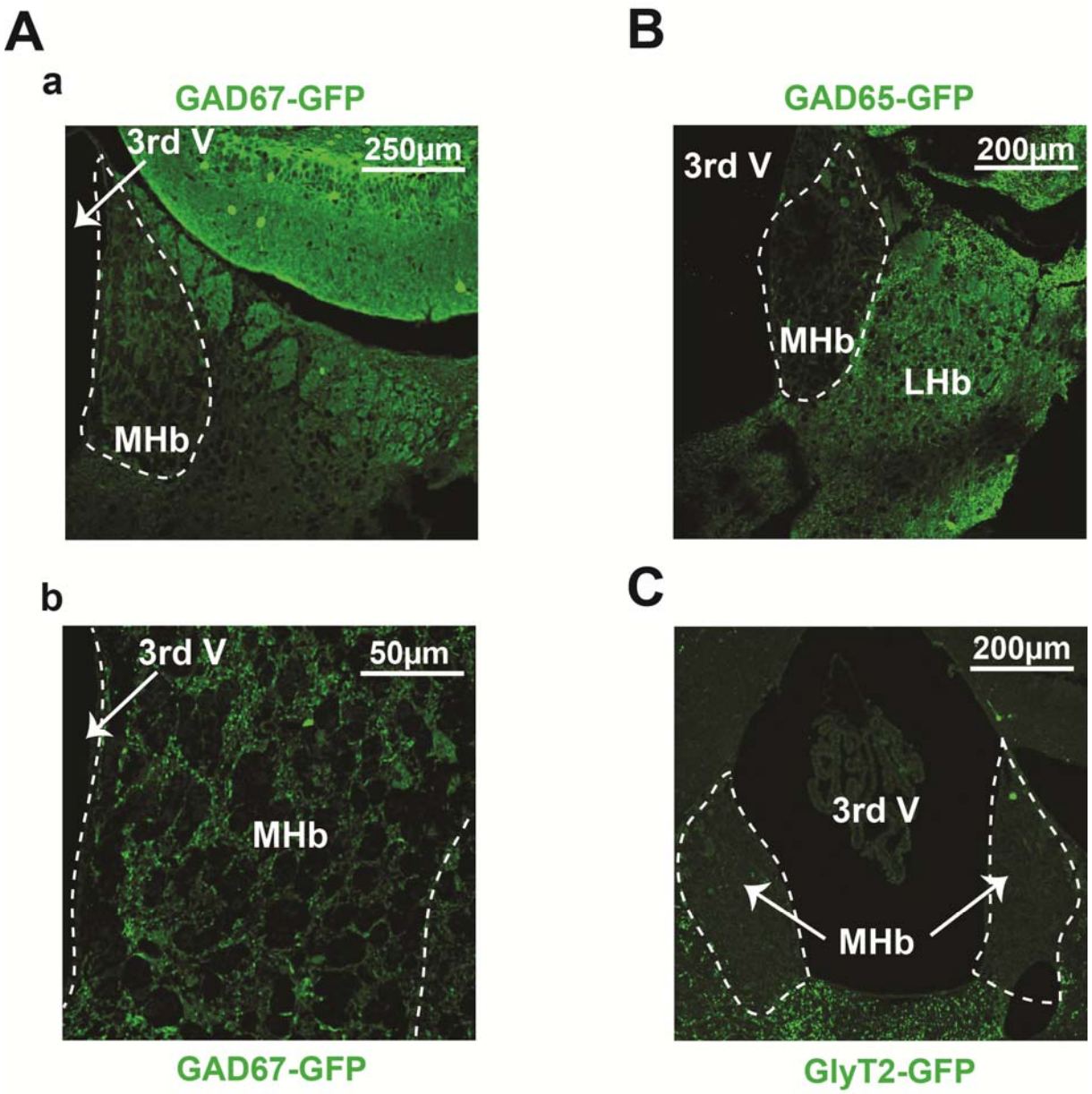

Figure S4 (related to Figure 6). The MHb is devoid of both GABAergic, and glycinergic local interneurons.

A. Typical GFP expression in the MHb and its surrounding regions of a coronal section from a GAD67-GFP mouse. In **a,** the low level of expression in the MHb can be compared with the dorsally located part of the hippocampus visible in the image. In **b,** at larger magnification, only the presence of putative axonal projections, most likely originating extrinsically from the medial septum (see Qin & Luo, 2009), can be detected. No local interneurons are present.

B. Here, a low magnification image of a coronal slice from a GAD65-GFP mouse is shown. Again, no local interneurons are present, the MHb being devoid also of the signal originating from the axonal plexuses of extrinsic origin found in GAD67-GFP mice. Note the difference in GFP level between the MHb, and the more laterally located lateral habenula (LHb).

C. Absence of both glycinergic cells and terminals in the MHb, as illustrated by a coronal section from a GlyT2-GFP animal. Note the difference of fluorescence between the MHb, and the dorsal part of the thalamic paraventricular nucleus, located just ventrally with respect to the third ventricle (3rd V; Giber et al., 2015).

Supplemental references

Borgius, L., Restrepo, C. E., Leao, R. N., Saleh, N. & Kiehn, O. 2010. A transgenic mouse line for molecular genetic analysis of excitatory glutamatergic neurons. *Mol Cell Neurosci,* 45**,** 245-57.

Giber, K., Diana, M. A., Plattner, V. M., Dugue, G. P., Bokor, H., Rousseau, C. V., Magloczky, Z., Havas, L., Hangya, B., Wildner, H., Zeilhofer, H. U., Dieudonne, S. & Acsady, L. 2015. A subcortical inhibitory signal for behavioral arrest in the thalamus. *Nat Neurosci,* 18**,** 562-8.

Glangetas, C., Girard, D., Groc, L., Marsicano, G., Chaouloff, F. & Georges, F. 2013. Stress switches cannabinoid type-1 (CB1) receptor-dependent plasticity from LTD to LTP in the bed nucleus of the stria terminalis. *J Neurosci,* 33**,** 19657-63.

Otsu, Y., Marcaggi, P., Feltz, A., Isope, P., Kollo, M., Nusser, Z., Mathieu, B., Kano, M., Tsujita, M., Sakimura, K. & Dieudonné, S. 2014. Activity-dependent gating of calcium spikes by A-type K+ channels controls climbing fiber signaling in Purkinje cell dendrites. *Neuron,* 84**,** 137-51.

Rousseau, C. V., Dugue, G. P., Dumoulin, A., Mugnaini, E., Dieudonne, S. & Diana, M. A. 2012. Mixed inhibitory synaptic balance correlates with glutamatergic synaptic phenotype in cerebellar unipolar brush cells. *J Neurosci,* 32**,** 4632-44.

Scofield, M. D., Boger, H. A., Smith, R. J., Li, H., Haydon, P. G. & Kalivas, P. W. 2015. Gq-DREADD Selectively Initiates Glial Glutamate Release and Inhibits Cue-induced Cocaine Seeking. *Biol Psychiatry,* 78**,** 441-51.

Vergnano, A. M., Rebola, N., Savtchenko, L. P., Pinheiro, P. S., Casado, M., Kieffer, B. L., Rusakov, D. A., Mulle, C. & Paoletti, P. 2014. Zinc dynamics and action at excitatory synapses. *Neuron,* 82**,** 1101-14.

Wang, H., Peca, J., Matsuzaki, M., Matsuzaki, K., Noguchi, J., Qiu, L., Wang, D., Zhang, F., Boyden, E., Deisseroth, K., Kasai, H., Hall, W. C., Feng, G. & Augustine, G. J. 2007. High-speed mapping of synaptic connectivity using photostimulation in Channelrhodopsin-2 transgenic mice. *Proc Natl Acad Sci U S A,* 104**,** 8143-8.